Title

A new human somatic stem cell from placental cord blood with intrinsic pluripotent differentiation potential.

Journal

The Journal of experimental medicine, 200(2)

ISSN

0022-1007

Authors

Kögler, Gesine
Sensken, Sandra
Airey, Judith A
et al.

Publication Date

2004-07-01

DOI

10.1084/jem.20040440

Peer reviewed

The Journal of Experimental Medicine

A New Human Somatic Stem Cell from Placental Cord Blood with Intrinsic Pluripotent Differentiation Potential

Gesine Kögler,[1] Sandra Sensken,[1] Judith A. Airey,[2] Thorsten Trapp,[1] Markus Müschen,[1] Niklas Feldhahn,[1] Stefanie Liedtke,[1] Rüdiger V. Sorg,[1] Johannes Fischer,[1] Claudia Rosenbaum,[3] Susanne Greschat,[3] Andreas Knipper,[1,4] Jörg Bender,[4] Özer Degistirici,[1,4] Jizong Gao,[5] Arnold I. Caplan,[5] Evan J. Colletti,[2] Graça Almeida-Porada,[6] Hans W. Müller,[3] Esmail Zanjani,[6] and Peter Wernet[1]

[1]*Institute for Transplantation Diagnostics and Cell Therapeutics, University of Düsseldorf Medical School, 40225 Düsseldorf, Germany*
[2]*Department of Pharmacology, University of Nevada Medical School, Reno, NV 89523*
[3]*Molecular Neurobiology Laboratory, Department of Neurology, University of Düsseldorf Medical School, 40225 Düsseldorf, Germany*
[4]*Kourion Therapeutics, 40764 Langenfeld, Germany*
[5]*Skeletal Research Center, Case Western Reserve University, Cleveland, OH 44106*
[6]*Veterans Administration Medical Center, University of Nevada, Reno, NV 89557*

Abstract

Here a new, intrinsically pluripotent, CD45-negative population from human cord blood, termed unrestricted somatic stem cells (USSCs) is described. This rare population grows adherently and can be expanded to 10^{15} cells without losing pluripotency. In vitro USSCs showed homogeneous differentiation into osteoblasts, chondroblasts, adipocytes, and hematopoietic and neural cells including astrocytes and neurons that express neurofilament, sodium channel protein, and various neurotransmitter phenotypes. Stereotactic implantation of USSCs into intact adult rat brain revealed that human Tau-positive cells persisted for up to 3 mo and showed migratory activity and a typical neuron-like morphology. In vivo differentiation of USSCs along mesodermal and endodermal pathways was demonstrated in animal models. Bony reconstitution was observed after transplantation of USSC-loaded calcium phosphate cylinders in nude rat femurs. Chondrogenesis occurred after transplanting cell-loaded gelfoam sponges into nude mice. Transplantation of USSCs in a noninjury model, the preimmune fetal sheep, resulted in up to 5% human hematopoietic engraftment. More than 20% albumin-producing human parenchymal hepatic cells with absence of cell fusion and substantial numbers of human cardiomyocytes in both atria and ventricles of the sheep heart were detected many months after USSC transplantation. No tumor formation was observed in any of these animals.

Key words: cord blood • regenerative medicine • ex vivo expansion • developmental potential

Introduction

Somatic human stem cells which can be propagated in large quantities while retaining their ability to differentiate into different tissue cell types could serve as a highly valuable resource for the development of cellular therapeutics (1). Although embryonic stem cells have the broadest differentiation potential (2), their use for cellular therapeutics is excluded for several reasons: the uncontrollable development of teratomas in a syngeneic transplantation model (3), imprinting-related developmental abnormalities (4), and

The online version of this article contains supplemental material.

Address correspondence to Gesine Kögler, Institute for Transplantation Diagnostics and Cell Therapeutics, Heinrich Heine University Medical Center, Moorenstrasse 5, Bldg. 14.80, 40225 Düsseldorf, Germany. Phone: 49-211-8116794. Fax: 49-211-8116792. email: koegler@itz.uni-duesseldorf.de

Abbreviations used in this paper: ALP, alkaline phosphatase; CB, cord blood; DAG, dexomethasone, ascorbic acid, β-glycerol phosphate; DAPI, 4-6′diamidino-2-phenylindoline; GABA, gamma amino butyric acid; GFAP, glial fibrillary acidic protein; hTau, human Tau protein; IBMX, isobuthyl methyl xanthine; MAPC, multipotent adult progenitor cell; MSC, mesenchymal stem cells; NF, neurofilament; NGF, nerve growth factor; NGS, normal goat serum; pd, population doubling; PFA, paraformaldehyde; TH, tyrosine-hydroxylase; USSC, unrestricted somatic stem cell.

 J. Exp. Med. © The Rockefeller University Press • 0022-1007/2004/07/123/13 $8.00
Volume 200, Number 2, July 19, 2004 123–135
http://www.jem.org/cgi/doi/10.1084/jem.20040440

ethical issues (1). On the other hand, previously published claims that adult tissue–specific stem cells possess an intrinsic differentiation potential to other tissues may have been premature. Over the past years, studies have shown that after hematopoietic allo-transplantation with BM or G-CSF–mobilized blood, a small percentage of donor cells can also be detected as nonhematopoietic tissue (5–9). However, this so-called "plasticity" appears to be an extremely rare event and may not carry a physiologically relevant impact in vivo (10). Moreover, subsequent data have shown that certain results may be the result of cell fusion (11). Recently, a rare cell from BM of rodents, called multipotent adult progenitor cell (MAPC), was identified which differentiated in vitro into cells of all three germ layers and contributed to most somatic tissues when injected into an early murine blastocyst (12). A phenotypically identical cell was isolated from human BM (13). It is unclear, however, whether such MAPCs decline with donor age, a phenomenon that has been observed for the hematopoietic (14) and the mesenchymal stem cell (MSC) compartment from BM (15). In contrast to adult BM, the stem cell compartment in cord blood (CB) is less mature. This has been documented for the hematopoietic stem cells, which in CB are more abundant than in BM and have a higher proliferative potential associated with an extended life span and longer telomeres (16–19). Besides this biological superiority, CB is abundantly available, is routinely harvested without risk to the donor, and infectious agents such as CMV are rare exceptions (20)—a definite advantage for the development of cell therapeutics in regenerative medicine. We identified a rare, CD45 and HLA class II–negative stem cell candidate displaying robust in vitro proliferative capacity without spontaneous differentiation but with intrinsic and directable potential to develop into mesodermal, endodermal, and ectodermal cell fates. Thus, we termed the primary population unrestricted somatic stem cell (USSC).

Materials and Methods

Generation and Expansion of USSCs. CB was collected from the umbilical cord vein with informed consent of the mother (21). USSCs were generated from 94 (40.3%) of 233 CB. The mononuclear cell fraction was obtained by Ficoll (Biochrom) gradient separation followed by ammonium chloride lysis of RBCs. Cells were plated out at 5–7 $\times$ 10^6 cells/ml in T25 culture flasks (Costar). Two different media were used to initiate growth of the adherent USSC colonies: myelocult medium (StemCell Technologies) and low glucose DMEM (Cambrex) with 30% FCS, dexamethasone (10^{-7} M; Sigma-Aldrich), penicillin (100 U/ml; Grünenthal), streptomycin (0.1 mg/ml; Hefa-pharma), and ultraglutamine (2 mM; Cambrex). Expansion of the cells was performed in the same media but with a lower concentration or in the absence of dexamethasone. Cells were incubated at 37°C in 5% CO_2 in a humidified atmosphere. When cells reached 80% confluency, they were detached with 0.25% trypsin (Cambrex) and replated 1:3 as outlined in Table S1 available at http://www.jem.org/cgi/content/full/jem.20040440/DC1. USSC karyotyping was performed by cytogenetic standard protocols.

Monoclonal Antibodies for Immunophenotyping of USSCs. FITC-conjugated Ab CD4 (13B8.2), CD8 (B9.11), CD11a (25.3.1), CD14 (RMO52), CD15 (80h5), CD31 (5.6E), CD33 (D3HL60), CD34 (581), CD44 (J-173), CD62L (DREG56), CD80 (MAB104), CD90 (F15.42), CD71 (YDJ122), HLA-ABC (B9.12.1), F(ab′)2 goat anti–mouse IgM/IgG, and isotype controls were from Beckman Coulter; CD45 (2D1), CD49b (AK7), CD86 (FUN-1), and CD40 (5C3) were from BD Biosciences; CD62E/P (1.2B6) were from Serotec; CD105 (SN6) was from Caltag; and CD106 (BBIG-V3) was from R&D Systems. PE-conjugated Ab CD11b (BEAR1), CD16 (3G8), CD25 (B1.49.9), CD29 (K20), CD38 (T16), CD49e (SAM1), CD50 (HP2/19), CD54 (84H10), CD56 (NKH-1), CD117 (95C3), and isotype controls were from Coulter; glycophorin A (GA-R2), CD10 (HI10a), CD13 (L138), CD49d (L25.3), CD49f (GoH3), CD73 (AD2), CD123 (9F5), CD166 (3A6), and HLA -DR (G46-6) were from BD Biosciences; and CD133/1 (AC133) and CD133/2 (AC141) were from Miltenyi Biotech. Unconjugated Ab CD58 (AICD58) and isotype controls from were Immunotech; FLK-1/KDR (A-3), cytokeratin 8 (C51), cytokeratin 18 (DC-10), CK8/18 (C51), and vimentin (V9) were from Santa Cruz; CD44H (2C5) was from R&D Systems; and human endo (P1H12) was from Chemicon. Goat anti–rat Cy2 and normal rat IgG were from Dianova. Analysis was performed on a Beckman Coulter EPICS XL-MCL.

RT-PCR Analysis of USSCs. RT reactions were performed at 50°C with Omniscript (QIAGEN) and the 3′ primers following supplier's instruction. The PCR reactions were performed with HotStar Taq Master Mix (QIAGEN) at 93°C for 5 min, 35 $\times$ 93°C for 30 s, 55°C for 30 s, 72°C for 1 min, and 72°C for 5 min. Expression of the following molecules was detected by RT-PCR: CD49e (5′-ggcttcaacttagacgcgg; 3′-ccaggttgatcaggtactc; 640 bp), CD105 (5′-cctgccactggacacagg; 3′-atggcagctctgtggtgttg; 411 bp), CHAD (5′-aggaaccagctgtccagct; 3′-agtcaccaggactggctg; 513 bp), PDGFRa (5′-acagtggagattacgaatgtg; 3′-cacatcagtggtgatctcag; 251 bp), EGFR (5′-tgccacaaccagtgtgct; 3′-gaccagttcatcagattcatc; 205 bp), IGFR (5′-cgagtggagaaatctgcgg; 3′-gaccagggcgtagttgtag; 272 bp), RUNX1 (5′-gcaagctgaggagcggcg; 3′-gaccgacaaacctgaggtc; 296 bp), and GAPDH (5′-ctcaagatcatcagcaatgcc; 3′-gatggtacatgacaaggtgc; 755 bp).

Telomere Length Measurement. Telomere length measurement was performed with the Telo TAGGG Telomere Length Assay (Roche Diagnostics) according to manufacturer's instructions. DNA was treated with RsaI and HinfI. Detection was performed with Image Master (Amersham Biosciences). Calculation of mean telomere restriction fragment lengths (mean TRF) was performed according to Harley et al. (22).

In Vitro Differentiation into Neural Cells. USSCs were seeded on glass coverslips coated with 1 mg/ml poly-D-lysine and 13 μg/ml laminin in differentiation medium XXL containing DMEM, 15% heat-inactivated FCS, 100 U/ml penicillin/streptomycin, 50 ng/ml nerve growth factor, 20 ng/ml bFGF, 1 mM dibutyryl cAMP, 0.5 mM isobuthyl methyl xanthine (IBMX), and 10 μM retinoic acid for up to 4 wk. For immunostaining, cells were fixed for 15 min with 4% paraformaldehyde (PFA). For immunostaining against gamma amino butyric acid (GABA) and tyrosine-hydroxylase (TH), cells were fixed in 4% PFA, 0.3% glutaraldehyde at RT for 5 min. After washing with PBS, cells were incubated in 1 M ethanolamine at RT for 20 min, preincubated and permeabilized in 10% normal goat serum with 0.03% Triton X-100 for at least 30 min, followed by incubation with the primary Ab (GABA 1:1000 (Sigma-Aldrich), TH 1:100 (Sigma-Aldrich), neurofilament (NF) cocktail 1:1,000 (BioTrend),

DOPA-decarboxylase 1:500 (Sigma-Aldrich), glial fibrillary acidic protein (GFAP) 1:300 (Chemicon), synaptophysin 1:100 (Sigma-Aldrich), and Na^+ channel 1:50 (Sigma-Aldrich). Secondary Ab were anti–mouse-FITC (1:100; Southern Biotechnology) and anti–rabbit rhodamine X Ab (1:1,000; Molecular Probes). Cell nuclei were labeled with 4-6′diamidino-2-phenylindoline (DAPI; Roche).

USSC Transplantation into the Hippocampus Region of Wistar Rats. USSCs were labeled with pKH26 (Sigma-Aldrich) according to the supplier's protocol 2 d before transplantation. Adult male Wistar rats were anesthetized with Rompun (5 mg/kg) (Bayer) and Ketavet (100 mg/kg) (Pharmacia Upjohn). For transplantation, animals received a single, unilateral stereotactic injection of 1 μl (75,000 USSC/μl) into the hippocampus region using a 22-gauge needle. Coordinates were set according to the atlas of Paxinos and Watson (23). The animals received immune suppression by s.c. injection of cyclosporin A (15 mg/kg Sandimmune; Novartis) for 10 d, starting with a double dose injection 1 d before surgery. At different time points after transplantation the animals were killed. The brains were immediately removed and frozen in methyl butane (Sigma-Aldrich) on dry ice. 20-μm coronal sections were cut through the brain using a freezing microtome (CM 3050; Leica). At intervals of ~400 μm, sections were stained for human Tau protein (hTau). Sections were fixed with 4% PFA for 10 min followed by 50%, 100%, 50% acetone (Merck), each for 2 min. After a washing step, sections were quenched by 0.3% H_2O_2 (Merck) for 30 min and blocked with 3% goat serum for 30 min. The hTau Ab (1:100; Chemicon) was incubated overnight at 4°C. After washes with PBS, sections were incubated with goat anti–rabbit biotinylated secondary Ab (1:200; Vector) for 1 h and rinsed with PBS. Later, sections were transferred to an avidin–biotin complex Vectastain ABC kit (Vector) and were developed with 3,3-diaminobenzidine (DAB; Sigma-Aldrich) and H_2O_2 for 10 min, dehydrated, and mounted in Entellan (Merck).

In Vitro Differentiation into Osteoblasts, Chondroblasts, and Adipocytes. For differentiation into osteoblasts, USSCs were plated at 8,000 cells/cm^2 in 24-well plates and at 70% confluency supplemented with 10^{-7} M dexamethasone, 50 μM ascorbic acid-2 phosphate, and 10 mM dexomethasone, asorbic acid, β-glycerol phosphate (DAG) (24). For Alizarin red staining, cells were fixed for 5 min with 70% ethanol at 4°C to determine calcium deposition. Alkaline phosphatase (ALP) activity was determined in cell lysates obtained by treating cell cultures with 1% Triton X-100. The ELISA-based method was performed according to the manufacturer's protocol (Sigma-Aldrich). Results are expressed in nmol of p-nitrophenol produced per min. For quantitative Ca^{2+} determination, cell layers were scraped off the dish in 0.5 N HCl according to manufacturer's instructions (Sigma-Aldrich). For chondrogenic differentiation, a micromass culture system was used (25). 2×10^5 USSCs were cultured in DMEM high glucose supplemented with antibiotic, 100 nM dexamethasone, 35 μg/ml ascorbic acid-2-phosphate, 1 mM sodium pyruvate, ITS + premix (1:100 dilution), and 10 ng/ml TGFβ1. Aliquots of 2×10^5 cells in 0.5 ml of medium were centrifuged at 150 *g* in 15 ml polypropylene conical tubes. The pelleted cells were incubated at 37°C and 5% CO_2 for 21 d. For Alcian blue staining, cell aggregates were fixed in 4% formalin and cut into 10-μm sections and stained for histology. For immunostaining, frozen sections were fixed with 100% ethanol, incubated in 0.2 U/ml chondrotinase ABC for 40 min at 37°C. Blocking of nonspecific Ab binding sites was performed in 5% BSA/PBS for 1 h. The sections were incubated with the primary Ab diluted in 0.5% BSA/PBS for 1 h. Collagen type II (Chemicon) was detected by fluorescence microscopy after incubation for 30 min with a FITC-labeled secondary Ab diluted in 0.5% BSA/PBS. To induce differentiation into adipocytes, cells were plated at 1,000 cells/cm^2 in 24-well plates in DMEM with 1 μM dexamethasone (Sigma-Aldrich), 10 μg/ml insulin, 0.5 mM IBMX (Sigma-Aldrich), and 100 μM indomethacin (Sigma-Aldrich) (26). After 2 wk of adipogenic stimulation, cells were fixed in 5% PFA for 30 min and incubated with Oil Red-O to stain lipid vacuoles.

In Vivo Differentiation into Bone and Cartilage. The surgical details of the femoral gap bone repair model were performed according to a method described by Bruder et al. (27), and differentiation into cartilage was shown previously (28).

In Vitro Differentiation into Hematopoietic Cells. 10^5 USSCs were expanded for 2 wk with 100 ng/ml Flt3-L (CellGenix), 100 ng/ml SCF (CellGenix), 100 ng/ml IL-3 (Cellsystems), 100 ng/ml IL-6 (CellSystems), 100 ng/ml TPO (CellGenix), and 100 ng/ml G-CSF (Amgen) in Myelocult medium as described previously (29). Human CFU assays were performed on days 0 and 14 (29) with 10^4 cells in Methocult (Stem Cell Technologies).

Detection of In Vivo Differentiation into Heart and Liver. Sheep heart was dissected into right and left atria, right and left ventricles, and septum. Several random strips from each area were fixed in 4% PFA, cut into 1 × 1-mm cubes, and embedded in OCT medium. 7–10-μm cryosections were probed with a human-specific anti–heat shock protein 27 (HSP27) Ab (Stressgen) (30) or the antidystrophin Ab NCL DYS2 (Novocastra) and anti–protein gene product 9.5 (PGP 9.5, ubiquitin c terminal hydroxylase) (Biogenesis). The secondary Ab for anti-HSP27 and antidystrophin was goat anti–mouse conjugated to Alexa 488, and the secondary Ab for anti-PGP 9.5 was goat anti–rabbit conjugated to Alexa 647 (Molecular Probes). Livers of the sheep were fixed in buffered formalin and embedded in paraffin. Liver sections (2 μm) were dewaxed and incubated for 10 min at 90°C for target retrieval. After blocking endogenous peroxidase by EnVision blocking reagent (Dako), sections were incubated in serum-free protein block (Dako) for 10 min and for 2 h in TBS containing 0.1% gelatin and the primary Ab anti–human serum albumin (clone HSA-11; 1:100; Sigma-Aldrich) or monoclonal anti–human hepatocyte Ab (clone OCH1E5; Dako). After washing, sections were incubated for 30 min with labeled polymer (EnVision System; Dako), and immunoreactivity was visualized by incubation with diaminobenzidine tetrahydrochloride. For microdissection applying the PALM Micro Beam System, immunohistochemistry was performed as described above with the monoclonal anti–human hepatocyte, clone OCH1E5 Ab except that sections were mounted on foil-laminated glass slides.

Single Cell PCR Analysis of Fusion/Cell Hybrids. Isolation of single cells of human origin from human and sheep chimera liver tissue sections with >20% human cells and single cells of ovine origin from chimera liver tissue sections were performed using the PALM Micro Beam System (P.A.L.M. Microlaser Technologies). After target cell identification (the chimeric sheep liver slides were stained previously with the human hepatocyte specific Ab) and dissection from the surrounding tissue by a nitrogen laser beam (LMM), another strong laser was used to catapult (LPC) the microdissected material directly into the tube cap containing 20 μl of PCR buffer (Promega). Before PCR amplifications, cells were digested by proteinase K as described (31). To analyze individual micromanipulated parenchymal liver cells from human liver and human (stained) and ovine (unstained) cells from chimeric sheep liver tissue, genomic fragments of the human V_H1, ovine V_H7 and human TCRVβ7.2 and ovine TCRCδ genes were amplified

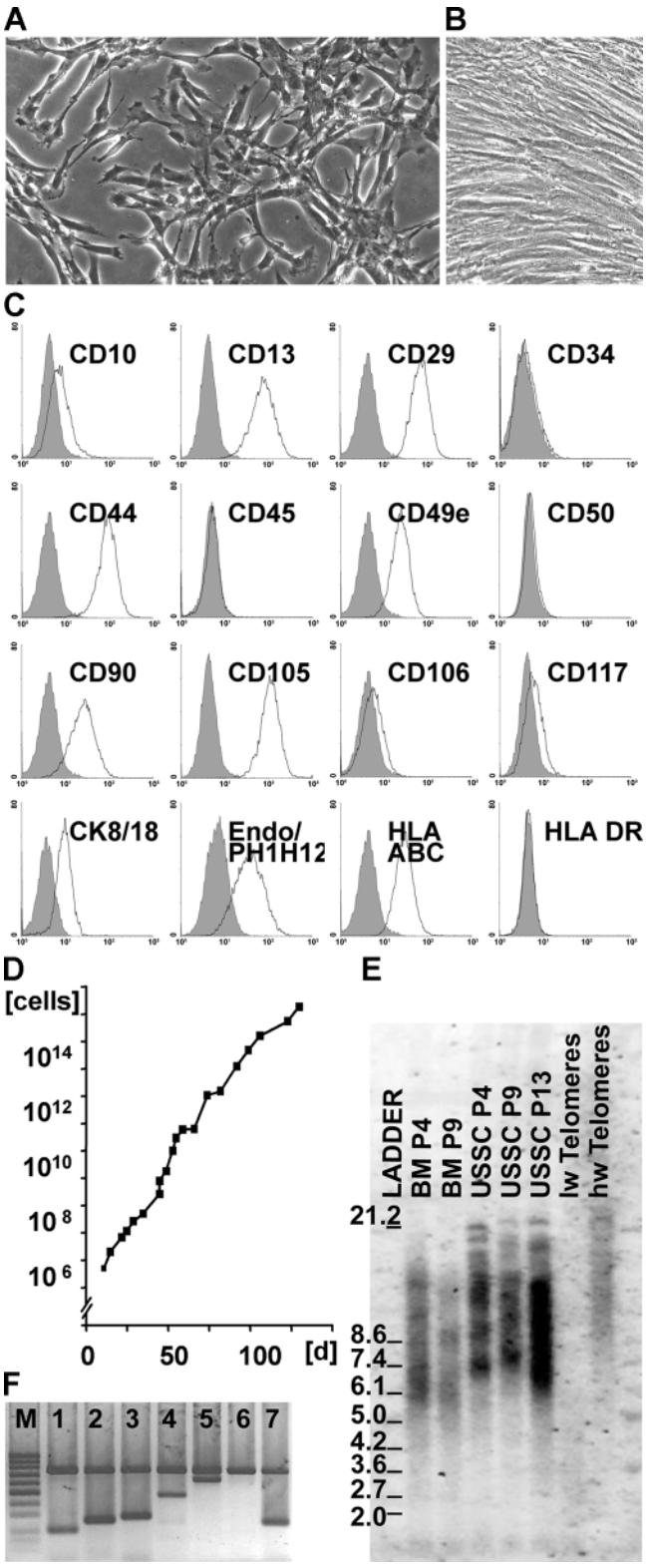

Figure 1. Characteristics of USSCs. (A) Spindle-shaped USSCs plated at low density after 32 population doublings (×20 magnification). (B) USSCs plated at high density after 24 population doublings (×20 magnification). (C) Immunophenotype of USSCs. Cells were labeled with the mAb specific for the molecules indicated (open histograms) or isotype controls (filled histograms). (D) Expansion kinetics of USSCs for 20 passages (p) equivalent to 46 population doublings (pd). (E) Expanded USSCs from CB have longer telomeres than MSCs from BM. Lane 1, ladder; lane 2, MSCs from BM, 19 pd (p4); lane 3, MSCs from BM, 27 pd (p9); lane 4, USSCs from CB, 21 pd (p4), lane 5, USSCs from CB, 25 pd (p9); lane 6, USSCs from CB, 36 pd (p13); lane 7 and 8, controls. Low weight (lw) and high weight (hw) telomeres were used according to manufacturer's instructions. (F) RT-PCR from undifferentiated USSCs: lane1, EGFR (205 bp); lane 2, IGFR (272 bp); lane 3, RUNX1 (296 bp); lane 4, CD105 (499 bp); lane 5, CD49e (640 bp); lane 6, CHAD (513 bp); lane 7, PDGFRa (251 bp). All reactions were coamplified with GAPDH (755 bp) as an internal positive control. All of these genes were expressed except for chondroadherin.

with all external primer pairs in a first PCR round. 1-μl aliquots from the first amplification round were then subjected to a second round of fully nested PCR amplification using internal PCR primers. The sequences of the primers used for PCR amplification are given in Table S2, available at http://www.jem.org/cgi/content/full/jem.20040440/DC1. Single-cell PCR amplifications were performed in a 60-μl reaction mix volume containing 2.5 mM $MgCl_2$ [Promega], 200 μM of each dNTP, 2.5 μM of each primer, 1× PCR buffer [Promega], and 2.5 U platinum Taq-polymerase (Invitrogen). Cycling conditions for the first round included a single 2-min denaturation step at 95°C followed by 34 cycles at 95°C for 1 min, 56°C for 30 s, and 72°C for 1 min, and a 5-min incubation at 72°C. For the second PCR round, 45 cycles of amplification were used. To rule out interspecies cross-reactivity of the primer pairs used, we also amplified DNA from ovine cells with human-specific primers and vice versa. Amplification products were analyzed by agarose gel electrophoresis.

Western Blot for Human Albumin. Serum proteins (human 50 ng/lane, ovine 500 ng/lane) were separated on a 12% SDS-polyacrylamide gel. After tank blotting onto a nitrocellulose membrane (Amersham Biosciences), blots were blocked with 5% blocking-grade nonfat dry milk (Amersham Biosciences) in PBS containing 0.05% Tween (PBS-T), incubated at 4°C for ~12 h with a human albumin-specific Ab (HAS-11, 1:5,000; Sigma-Aldrich). After five washes for 5 min in PBS-T, blots were incubated with horseradish peroxidase–coupled anti–mouse secondary Ab (1:2,000; Amersham Biosciences) at RT for 1 h. Membranes were washed again and developed using the Amersham Biosciences ECL system according to manufacturer's instructions.

Online Supplemental Material. Expansion kinetic of USSCs (cell numbers, passages, and population doublings) are shown in Table S1. The sequences of the primers used for PCR amplification in the single cell PCR analysis of fusion/cell hybrids of the chimeric liver tissue are given in Table S2. Tables S1 and S2 are available at http://www.jem.org/cgi/content/full/jem.20040440/DC1.

Results

Isolation, Expansion, and Characterization of USSCs from Placental CB. USSCs were generated from 94 CB samples of a mean gestational age of 39.5 ± 1.46 wk (range 34–42), a net volume of 80 ± 21.4 ml including 29 ml citrate-phosphate dextrose (range 43–140 ml) and a total nucleated cell count of 7.6 ± 3.1 × 10^8 (range 2.4–19.4). No correlation was detected between gestational age (>30 wk), hours elapsed after CB collection, volume, number of mononuclear cells in the CB after gradient separation and the success in generation of USSC. After 6–25 d (mean 15 d), adherently growing cells (USSC colonies) of fibroblastic morphology were detected with a median frequency of four colonies per

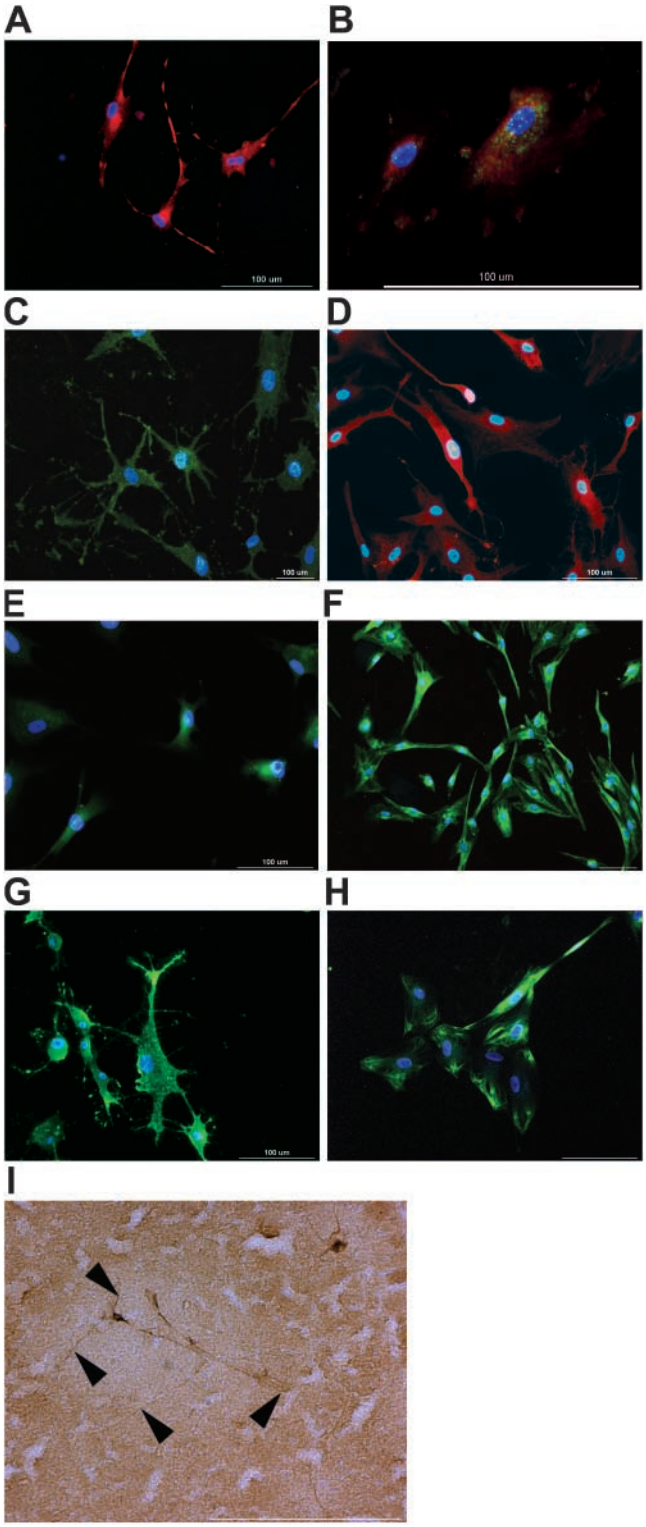

Figure 2. In vitro and in vivo differentiation of USSCs into neural cells. In XXL, medium differentiated cells showed positive immunoreactivity for the neuron-specific marker NF (A), voltage-gated sodium channels (green) coexpressed with NF (red) (B) for synaptophysin, a protein located in the synaptic vesicles of neurons (C), the inhibitory neurotransmitter GABA (D), the enzymes TH (E), DOPA-decarboxylase (F), and choline acetyltransferase, the enzyme of the cholinergic pathway (G), and the astrocyte-specific marker GFAP (H). Cell nuclei show a blue color due to DAPI staining. USSCs staining positively for hTau in the ipsilateral cortex 3 mo after stereotactic implantation into the hippocampus region (I). Note the long processes (indicated by arrowheads) and the highly differentiated neuronal like morphology. Bars, 100 μm.

CB (range 1–11). As shown in Fig. 1, A and B, USSCs are adherent, spindle-shaped cells, and have a size of 20–25 μm. Hematopoietic $CD45^+$ cells were no longer detected after three passages. The USSC karyotype was normal 46XX or 46XY as analyzed for six individual USSC specimens for passages 5 (21 population doublings) to 19 (45 population doublings). USSCs were negative for CD14, CD33, CD34, CD45, CD49b, CD49c, CD49d, CD49f, CD50, CD62E, CD62L, CD62P, CD106, CD117, glycophorin A, and HLA-DR and expressed high levels of CD13, CD29, CD44, CD49e, CD90, CD105, vimentin, and cytokeratin 8 and 18, human Endo, low levels of CD10, and FLK1 (KDR), and showed variable but weak expression of HLA-ABC (Fig. 1 C). USSCs can be cultured for >20 passages equivalent to >40 population doublings without any spontaneous differentiation (Fig. 1 D and Table S1). The average telomere length of USSCs obtained after both 21 (passage 4) and 25 population doublings (passage 6) was 8.93 kbp; after 36 population doublings, the average telomere length of USSCs obtained was 8.60 kbp (passage 13). This is significantly longer than the telomere length of MSCs generated from a BM donor (age 30 yr) with 7.27 (passage 4) and 7.11 kbp (passage 9) at 19 and 27 population doublings, respectively (Fig. 1 E). USSCs showed expression of transcripts for epidermal growth factor receptor, platelet-derived growth factor receptor, insulin-like growth factor receptor, runt related transcription factor (Runx1), YB1, CD49e, and CD105 (Fig. 1 F). They were negative for the chondrogenic extracellular protein chondroadherin (Fig. 1 F), the bone-specific markers collagenase X, bone sialoprotein, the liver and pancreas-specific markers Cyp1A1 and PDX-1, and neural markers such as NF, synaptophysin, TH, and glial fibrillary acid protein (not depicted). Preliminary cDNA microarray analysis performed for two individual USSCs and one MSC preparation from human BM suggested differential expression of HAS1, which was only detected in MSCs but not in USSCs. This differential expression of HAS1 was confirmed by RT-PCR ($n = 55$; unpublished data) and immunochemistry.

Differentiation into Neural Cells In Vitro and In Vivo. Individual USSC preparations ($n = 10$) from passages 3–16 were analyzed for their neural differentiation potential. In XXL medium, the number of NF-positive cells increased, starting with ~30% after 1 wk to more than 70% homogeneity after 4 wk (Fig. 2 A). Double immunostaining revealed colocalization of NF and sodium-channel protein in a small proportion of cells (Fig. 2 B). Expression of synaptophysin was detected after 4 wk (Fig. 2 C), indicating a more mature phenotype of neurons. Consistently, ~90% of the cells stained positive for the inhibitory neurotransmitter GABA (Fig. 2 D). USSC-derived neurons could be identified that stained positive for TH (~30% of the cells), the key enzyme of the dopaminergic pathway (Fig. 2 E). On

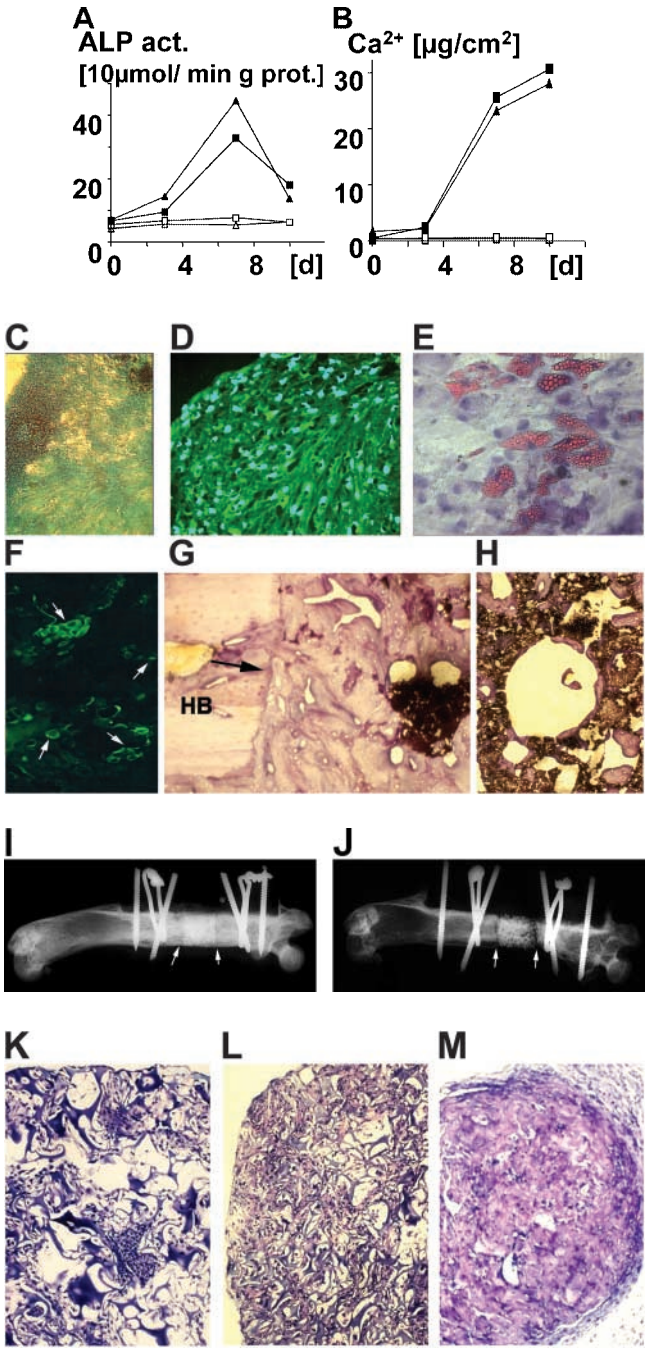

Figure 3. In vitro and in vivo differentiation of USSCs into osteoblasts, chondroblasts, and adipocytes. (A) Differentiation to osteoblasts is shown by the ALP assay. The peak of ALP was already achieved on day 7. Both basic media McCoy (filled square) and DMEM (filled triangle) in the presence of DAG were able to support the osteoblast differentiation. USSCs (control: open triangle, DMEM; open square, McCoy) cultured without DAG showed no ALP activity. (B) Quantitative Ca^{2+} release assay. Both basic media McCoy (filled square) and DMEM in the presence of DAG (filled triangle) were able to support the osteoblast differentiation. USSCs (control: open triangle: DMEM; open square, McCoy) cultured without DAG showed no Ca^{2+} activity. (C and D) Chondrogenic differentiation. (C) Demonstrates an Alcian blue–positive extracellular matrix at day 21 after stimulation toward the chondrogenic pathway, indicating a homogeneous distribution of sulfated proteoglycans within the matrix structure (×10 magnification). (D) Collagen type II staining of pellet microsections analyzed by fluorescence microscopy; the nuclei are stained with DAPI (×40 magnification). (E) Oil Red-O staining of the lipid vesicles performed 2 wk after stimulation demonstrates an ongoing adipogenesis (×40 magnification). In vivo differentiation of USSCs into bone and cartilage. (F–M) Ceramic cylinders were loaded with USSCs and transplanted into nude rat femur critical size defects of 0.5 cm in length. (F) 4 wk after transplantation, human cells were still present in the bone defect as demonstrated by immunohistochemical staining with the human-specific mAb 6E2 (×20 magnification). (G and H) Images of the longitudinal (G) and cross section (H) demonstrate bony healing between the cell-loaded implant and the host bone (HB). Bony integration was established in forms of cancellous bone as detected by Toluidine blue staining (×4 magnification). (I) Faxitron high resolution x-ray scanning of specimens harvested at 12 wk after surgery demonstrates the healing between the cell-loaded implant and the host bone (magnification, original size). (J) Unloaded ceramic cylinders served as negative controls demonstrating a nonhealing between the scaffold and the host bone. Arrows indicate the interface between the scaffold and the host bone (magnification, original size). (K–M) A successful in vivo chondrogenesis of USSC-loaded Gelfoam sponges in a nude mouse model. Human USSCs loaded into gelatin sponges were cultured in vitro for 1 (K) or 2 (L) wk in a chondrogenic medium with TGF-β. These sponges were s.c. implanted into nude mice for another 3 wk before analysis. At 1 (K) or 2 (L) wk of in vitro culture, cells filled the pores of the Gelfoam sponge. Some local spots demonstrate an extracellular matrix formation which indicate chondrogenic lineage differentiation. The implanted cells demonstrate strong chondrogenic differentiation as documented by Toluidine blue staining (M) (×10 magnification).

the other hand, the number of DDCs (Fig. 2 F), the subsequent enzyme of the same transmitter pathway, was highly variable. Choline acetyltransferase, the enzyme of the cholinergic pathway, was detected in ∼50% of the cells (Fig. 2 G). Since 90% of USSCs in vitro showed positive immunoreactivity for GABA, coexpression with the enzymes of other neurotransmitter pathways was observed. These findings could be explained by the function of GABA during very early embryogenesis, where it is described to act as a signal molecule in neuronal development (32). Extensive analyses by patch-clamp recording of different USSC batches did not thus far reveal a voltage-activated, fast inactivating Na^+ current, which is typical of terminally differentiated neurons (Copi, A., and K. Gottmann, personal communication). This finding suggests that USSCs differentiate to a precursor-like phenotype in vitro, in which distinct neuron-specific proteins are expressed, but a fully functional neuronal phenotype has not yet developed. Moreover, USSCs differentiated into astrocytes expressing GFAP, an astroglial intermediate filament reaching a transient maximum level of ∼45% at 2–3 wk in XXL medium (Fig. 2 H). During early differentiation, coexpression of GFAP and NF could be observed, indicating a common progenitor cell type (unpublished data). Interestingly, after 2–3-wk GFAP immune reactivity declined resulting in a more enriched neuronal cell population. To analyze the potency of USSCs to migrate, integrate, and differentiate into neuronal-like cells in vivo, USSCs were labeled with pKH26 and transplanted stereotactically into the hippocampus region of an intact adult rat brain. Numerous pKH26-labeled cells could be detected after 3 mo postgrafting (unpublished data). At 3 mo postimplantation, USSCs expressing human Tau protein could be identified widely distributed throughout the brain, indicating a high migratory activity of USSCs in vivo.

Human Tau immune staining further revealed the neuronal-like, highly differentiated morphology of implanted USSCs in different ipsi- and contralateral regions of the adult brain including the neocortex (Fig. 2 I). In the brain of a nongrafted control animal, no human Tau immunoreactivity could be detected (unpublished data).

In Vitro Differentiation of USSCs into Bone, Cartilage, and Adipocytes. All USSCs tested ($n = 30$; up to passage 21) were capable of differentiating along the osteogenic and chondrogenic lineage. Adipogenic differentiation was observed for all six USSCs tested. Differentiation into osteoblasts was induced by dexamethasone, ascorbic acid, and DAG. After 5 d, cells showed initial calcium phosphate deposits. Bone-specific ALP activity was detected (Fig. 3 A) and continuous increase in Ca^{2+} release was documented (Fig. 3 B). Osteogenic differentiation was confirmed by expression of ALP, osteocalcin, osteopontin, bone sialo-protein, and collagen type I detected by RT-PCR (unpublished data). A pellet culture technique was employed to trigger USSCs toward the chondrogenic lineage (25). The chondrogenic nature of differentiated cells was assessed by Alcian blue staining (Fig. 3 C) and by expression of the cartilage extracellular protein type II collagen (Fig. 3 D). Chondrogenesis was further confirmed by RT-PCR for the cartilage-specific mRNAs encoding Cart-1, collagen type II, and chondroadherin (unpublished data). For induction of adipogenic differentiation, USSCs were cultured with dexamethasone, insulin, IBMX, and indomethacin (26). Adipogenic differentiation was demonstrated by Oil Red-O staining of intracellular lipid vacuoles (Fig. 3 E).

In Vivo Differentiation of USSCs into Bone and Cartilage. To determine the in vivo regeneration capacity for bone, the repair of critical size bone defects with USSC-loaded calcium phosphate ceramic cylinders was demonstrated. USSCs ($n = 7$) were expanded to passage 5 and loaded into porous ceramic cylinders of 5-mm length before implantation into the femur critical size bone defect of athymic Harlan Nude rats. 4 wk after transplantation, human cells were still alive within the defect bone (Fig. 3 F). Images of longitudinal (Fig. 3 G) and cross sections (Fig. 3 H) demonstrated bony healing between the cell-loaded implant and the host bone. Bony integration was established in forms of cancellous bone as detected by Toluidine blue staining. After 12 wk, a clear bony reconstitution was observed (Fig. 3 I). Cell-free implants served as negative controls (Fig. 3 J). However, it is impossible to quantitatively assess the number of human cells in the responding zone, since serial section reconstruction was not performed. Moreover, as shown by Allay et al. (33) the human cells initiate the fabrication of lamellar bone in implanted ceramic vehicles, but since the osteoblasts half-lives are 8–10 d, eventually the momentum of bone formation is joined by host-derived cells. However, the observation shown here indicates that the USSCs initiated the bone formation in the orthotopic site. The in vivo chondrogenic potential was assayed by loading USSCs into gelatin sponges (4×4 mm, Gelfoam®; Upjohn Pharmacia). They were cultured in chondrogenic medium with supplementation of TGF-β (5 ng/ml) for up to 2 wk (Fig. 3, K and L) and then implanted s.c. into nude mice. After an additional 3 wk, the implanted cells demonstrated strong chondrogenic differentiation as shown by Toluidine blue staining (Fig. 3 M).

In Vivo and In Vitro Differentiation of USSCs into Hematopoietic Cells. To evaluate the potential of USSCs to differentiate in vivo into hematopoietic cells, in utero transplantation into fetal sheep was employed (34). USSCs were transplanted intrauterine before immunological maturity. USSCs originating from one expanded colony tested negative for the human hematopoietic antigen CD45 by flow cytometry and PCR and were injected i.p. (1,500 USSC/sheep) into six preimmune (day 57–62) fetal sheep. To determine donor cell engraftment, blood and BM cells were analyzed by flow cytometry for the presence of human cells as described previously (35). Multilineage hematopoietic engraftment was observed, which included cells of erythroid (glycophorin A), myeloid (CD13, CD33), and lymphoid (CD3, CD7, CD10, CD20) lineages. Four out of six animals showed clear evidence of human hematopoietic reconstitution (up to 5% human hematopoietic and lymphopoietic engraftment in the total nucleated cell fraction in the blood after RBC lysis) 4-mo posttransplantation (Table I). The level of these human cells in the BM of these sheep was maintained through 12 mo posttransplant. In an attempt to elucidate these primarily unexpected in vivo results in vitro, 10^4 and 10^5 USSCs ($n = 14$; passages 5–8) were plated directly into a standard CFC assay. However, immediate hematopoietic colony formation was not observed for any of the 14 USSC preparations. When 10^5 USSCs ($n = 14$) were cultured for 2 wk in the presence of hematopoietic growth factors, the cell number decreased to 3×10^4 cells (range $2.0–3.4 \times 10^4$). When these growth factor pretreated cells were subjected to the same standard CFC assay with 10^4 total cells, in 2 of 14 USSC preparations hematopoietic CFC were observed, but the frequency of two and six colonies per 10^4 seeded USSCs was very low. Since the morphology of such CFC was slightly different than that of regular CFC in CB or BM, the USSC-derived CFCs were pooled and analyzed by flow cytometry. The expression of glycophorin A (Fig. 4, 2.7%) and CD33 (Fig. 4, 85%) on these colony-derived cells confirmed the hematopoietic nature.

In Vivo Differentiation of USSCs into Myocardial Cells and Purkinje Fibers. To explore the in vivo differentiation potential of USSCs into myocardial cells, the preimmune fe-

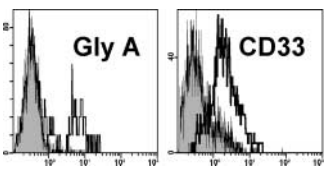

Figure 4. In vitro hematopoiesis of USSCs. Glycophorin A (PE-conjugated Ab) staining of the colonies for confirmation of erythroid progenitor cells and CD33 staining (FITC-conjugated Ab) of the colonies for the detection of myeloid progenitor cells. mAb specific for the molecule indicated (open histograms) or isotype controls (filled histograms).

Table I. *Hematopoietic Cell Chimerism After Human USSC in Utero Transplantation into Fetal Sheep*

Antibody	Blood 4 mo[a] post-TPX	Bone marrow 4 mo[a] post-TPX	Bone marrow 5 mo[b] post-TPX	Bone marrow 12 mo[b] post-TPX
CD45	1.66 (0.06–4.68)	0.09 (0.06–0.12)	1.42 (1.10–1.90)	2.75 (1.80–4.20)
CD34	0.00 (0.00–0.00)	0.14 (0.00–0.40)	0.09 (0.07–0.14)	0.18 (0.13–0.20)
Glycophorin A	4.45 (2.63–6.50)	2.26 (1.72–2.67)	3.02 (1.20–5.20)	2.30 (0.00–4.20)
CD7	0.59 (0.41–0.78)	2.23 (0.95–4.04)	1.85 (0.90–3.00)	2.70 (1.10–4.90)
CD3	0.44 (0.00–0.89)	0.29 (0.00–0.89)	0.37 (0.00–0.90)	1.08 (0.90–1.30)
HLA-DR	3.07 (0.67–6.68)	0.35 (0.00–1.05)	ND	ND
CD10	0.15 (0.08–0.29)	0.06 (0.00–0.14)	ND	ND
CD33	0.00 (0.00–0.00)	0.01 (0.00–0.04)	ND	0.70 (0.00–1.40)
CD13	0.06 (0.00–0.15)	0.01 (0.00–0.02)	ND	ND
CD20	0.00 (0.00–0.00)	0.00 (0.00–0.00)	0.15 (0.00–0.30)	0.52 (0.00–0.60)

Each fetus was transplanted with 1,500 cells. Please note that the values for some markers together (HLA-DR; CD7, CD3) exceed those of CD45. The up and down regulation of CD45 on different cell populations in this xenogeneic model was described previously (49). ND, not done.
[a]$n = 3$ animals were analyzed; mean (range) values in percentages are presented.
[b]$n = 4$ animals were analyzed; mean values in percentages are presented.

tal sheep model was applied as described above. Differentiation of USSCs into human cardiomyocytes was analyzed 8 mo after transplantation. We have demonstrated previously the strict human specificity of the anti-HSP27 in sheep heart (30). Positive staining with the human-specific anti-HSP27 Ab was found in both atria, both ventricles, and the septum of the heart of in utero USSC-transplanted sheep, indicating that in this developmental in vivo model USSCs can robustly engraft throughout the heart (Fig. 5, A and B). Within the cells displayed in the longitudinal tissue section (Fig. 5 A), the HSP27 staining shows a striped pattern, which is consistent with previous findings (36). To demonstrate that the cells labeled with the human-specific HSP27 Ab were mature cardiomyocytes, tissue sections were probed with several antibodies that have a distinctive staining in cardiac cells. These antibodies employed had a broad specificity so that they could be used to confirm that this staining pattern was identical for the cells derived from the USSCs and from the surrounding cardiac sheep cells. Antibodies included antiryanodine receptor, anti-MHC, and as shown in Fig. 5, C and D, antidystrophin. In the adult heart, dystrophin is expressed at significant levels and localized at the plasma membrane (37, 38). As can be seen, both engrafted human cells and sheep cells have the mature pattern of distribution of dystrophin and are indistinguishable. The distribution pattern of HSP27 (Fig. 5 A) and other proteins such as dystrophin (Fig. 5, C and D) indicate that the engrafted human cells have a mature cardiac phenotype and the correct localization of proteins to be functional cardiomyocytes. The distribution of the engrafted cells observed was not homogeneous throughout the heart. In certain areas only single HSP-27–positive cardiomyocytes were detected, whereas in other areas groups of positive human cardiomyocytes were interspersed with sheep cardiomyocytes (Fig. 5 E). In some areas the engrafted cells were found in patches, with 10–20% of the cells in these areas being human cardiomyocytes interspersed with sheep cardiomyocytes. These quantities ranged from 0–3% of the sections analyzed ($n = 30$); however, in the atria and ventricle-positive patches of up to 10–20% USSC-derived cells were found. There was no pattern in the distribution, such as proximity to blood vessels. Using the preimmune fetal sheep model, we had shown previously that human MSCs from both fetal and adult sources engraft predominantly in the Purkinje fiber system and there are very few human cardiomyocytes (30). In this study, engraftment of USSCs in the Purkinje fiber system was detected also. Identification was by the characteristic morphology and staining with the characteristic Purkinje fiber marker PGP 9.5 (30). Similar to our earlier demonstration in preimmune sheep injected with human MSC, the engrafted human cells derived from USSCs were found in aggregates (Fig. 5 F) and not interspersed with sheep Purkinje fiber cells. This result is in contrast to the engrafted human cardiomyocytes, which are interspersed with the sheep cardiomyocytes.

In Vivo Differentiation of USSCs into Hepatic Cells. To examine human hepatocyte development, livers of the sheep were taken 14-mo post-USSC transplantation. Fig. 6 A shows the specific staining of the human hepatocyte Ab OCH1E5 with a human liver. A liver from a nontransplanted sheep showed no cross-reactivity with the human-specific Ab (Fig. 6 D). As shown in Fig. 6 C in close association with portal veins, donor parenchymal liver cells generated from the USSCs represent the majority of total hepatic cells. Counting of representative areas of tissue sections of chimeric sheep liver revealed that 21.1 ± 3.2% of total liver cells were stained positive by the Ab that specifi-

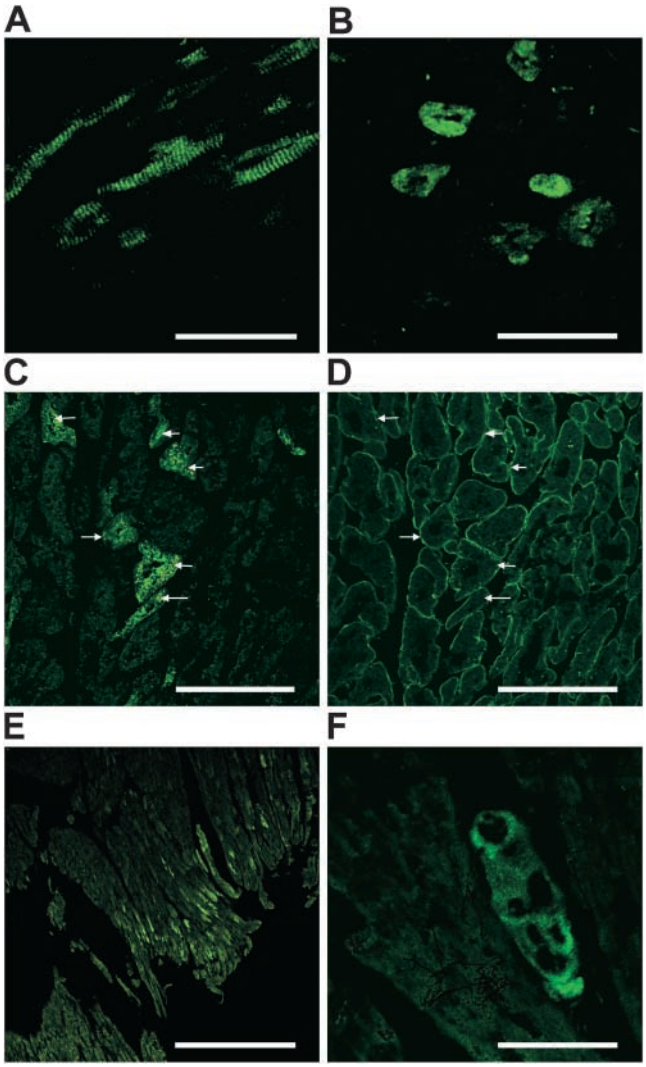

Figure 5. In vivo differentiation of USSCs to cardiomyocytes and Purkinje fibers. (A and B) Groups of engrafted cells in the right atria in a longitudinal section (A) and from the right ventricle in a cross section (B) stained with human-specific anti-HSP27. (C and D) Serial sections of the right ventricle. C is labeled with a human-specific anti-HSP27 mAb, and D is labeled with an antidystrophin mAb with broad species specificity. Arrows indicate the same cells. (E) An area from the left ventricle showing areas of engrafted human cells surrounded by sheep cells. (F) A section of Purkinje fiber labeled with the human-specific anti-HSP27. Bars: (A–E) 50 μm; (F) 100 μm.

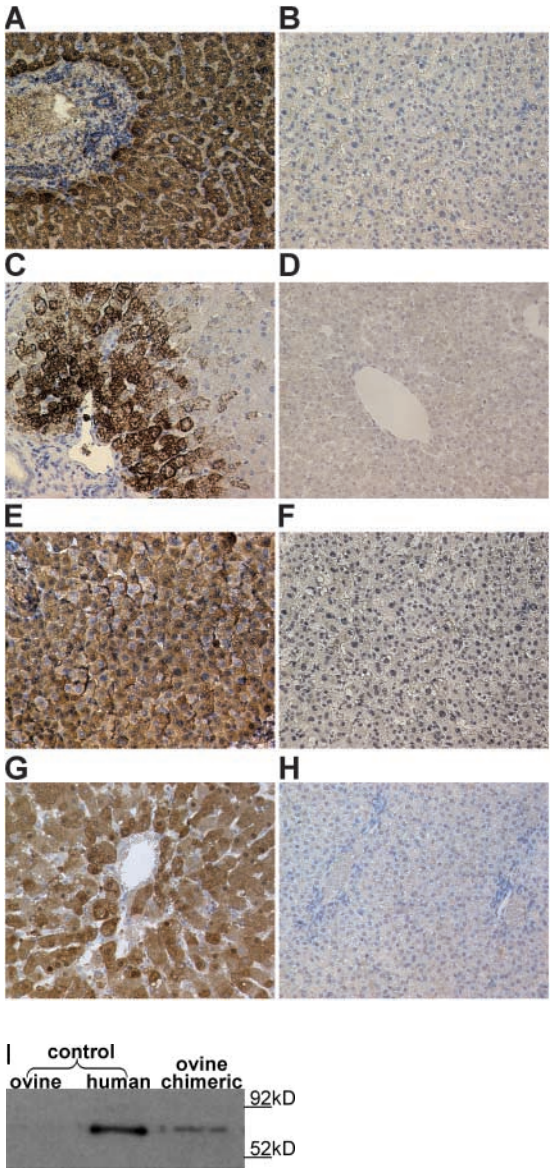

Figure 6. In vivo differentiation of USSCs from CB into parenchymal liver cells in the preimmune fetal sheep model. (A) Positive control: human liver stained with the anti–human hepatocyte Ab. The specificity for parenchymal liver cells is shown, since fibroblasts and endothelial cells in association with the portal spaces are negative. (B) Negative control: human liver stained with only the second Ab; no reaction or unspecific staining was observed. (C) Photomicrographs show the staining for the anti–human hepatocyte Ab in liver sections of animals transplanted with USSCs; in close association with the portal veins >80% of cells stained positive. No vessels are stained. (D) Negative control: the liver of a normal sheep shows no reaction with the Ab specific for human hepatocytes (A–D, × 20 magnification). (E–H) The anti–human albumin staining of the liver. E is the positive control: the human liver stained positive with the mAb HSA-11. (F) The human liver stained with only the second Ab: no reaction or unspecific staining was observed. (G) The staining of the anti–human albumin Ab in liver sections of animals transplanted with USSCs. (H) Liver of a normal sheep showed no reaction with the human albumin. (E–H, ×20 magnification). (I) Western blot of human albumin in human serum and serum of chimeric and control sheep. A representative Western blot is shown.

cally recognizes human hepatocytes in association with portal veins >80%. To use a different human-specific Ab, the mAb HSA-11 recognizing human albumin was applied, which shows a specific staining for the human liver (Fig. 6 E) and no reactivity with the sheep liver (Fig. 6 H). In contrast, the liver of the sheep transplanted with USSCs showed a strong staining with human albumin (Fig. 6 G). Since human albumin is a secreted protein, the majority of cells stained positive, some showed a very strong pattern of albumin distribution, and the ones in the periphery showed a weaker staining. Fig. 6 I reproduces a Western blot showing

a specific human albumin band and thus the functional production of this human protein in vivo in serum of the sheep obtained 17 mo after transplantation of the USSCs in utero.

Cell Fusion Does Not Account for Liver Cell–specific Differentiation of USSC. To determine whether the human cells integrated into the sheep liver parenchyma acquired an organ-specific differentiated phenotype through cell fusion with indigenous ovine liver parenchymal cells or by liver cell differentiation, we tested single microdissected liver parenchymal cells from chimeric liver tissue for the coexistence of human and ovine genomes in these cells. To this end, single liver parenchymal cells, in which either expression of human proteins could be detected or were devoid of human proteins, were micromanipulated from chimeric liver sections and separately analyzed by single cell PCR. Each cell was transferred into a PCR reaction tube, digested by proteinase K, and subjected to two rounds of nested PCR amplification using four sets of human and sheep DNA–specific primers. To check for potential interspecies cross-reactivity of these primer sets specific for *IGH* and *TCR* loci of either human or sheep origin, we microdissected single liver parenchymal cells from human liver tissue sections as a control. From one third of the microdissected cells, we obtained a human PCR product but not a single PCR product of sheep origin. While analyzing 80 cells from chimeric tissue prestained with the human hepatocyte-specific Ab OCH1E5, human DNA fragments originating from the human *IGH* or *TCRB* loci and sheep DNA fragments from ovine *IGH* and *TCRD* loci were coamplified. In 24 of these 80 cells derived from paraffin sections, amplification gave rise to a PCR product for human DNA, whereas not a single sheep-specific PCR product was detected (Table II). Conversely, coamplification of human and ovine DNA fragments from cells micromanipulated from chimeric tissue, which did not stain for human proteins, only yielded PCR products of ovine but not human DNA (Table II). Using 16 PCR reactions, to which only PCR buffer but no cells were added as negative controls, neither human nor ovine DNA could be amplified. We conclude that fusion events, if they occur at all under physiological noninjury conditions, at best could account at a very low frequency for the differentiated liver cell–specific phenotype of the USSC-derived hepatocytes integrated into the chimeric liver tissue.

Discussion

In this study, an adherent CD45-negative unrestricted stem cell population from human placental CB was shown to be pluripotent. In contrast to other data from CB identifying mesenchymal cells that differentiated only into osteoblasts, chondrocytes, adipocytes (39, 40), or neural progen-

Table II. *Summary of Single Cell PCR Analysis of Micromanipulated Cells Revealing Complete Absence of Cell Fusion Events in This Noninjury Model*

Gene locus	Tissue	Staining	Positive cells	Buffer controls
Human V_H1	Human	Positive	8/24	
Human V_H1	Chimera	Negative	0/24	
Human V_H1	Chimera	Positive	22/80	0/16
Human TCRVβ7.2	Human	Positive	8/24	
Human TCRVβ7.2	Chimera	Negative	0/24	
Human TCRVβ7.2	Chimera	Positive	21/80	0/16
Σ	Human	Positive	8/24	
Human V_H1 or TCRVβ7.2	Chimera	Negative	0/24	
	Chimera	**Positive**	**24/80**	**0/16**
Ovine V_H7	Human	Positive	0/24	
Ovine V_H7	Chimera	Negative	9/24	
Ovine V_H7	Chimera	Positive	0/80	0/16
Ovine TCRCδ	Human	Positive	0/24	
Ovine TCRCδ	Chimera	Negative	9/24	
Ovine TCRCδ	Chimera	Positive	0/80	0/16
Σ	Human	Positive	0/24	
Ovine V_H7 or TCRCδ	Chimera	Negative	9/24	
	Chimera	**Positive**	**0/80**	**0/16**

itors in vitro (41), this is the first time that an adherent cell population has been identified, which after ex vivo expansion allows directed differentiation into bone, cartilage, hematopoietic cells, neural, liver, and heart tissue in vivo in various animal models. Previously, even the existence of mesenchymal/mesodermal cells in term CB has been very controversial. Several groups were unable to generate MSCs (42, 43) or generated MSCs only in a limited number of CB specimens (39, 41). Although the USSCs described here have a very low primary frequency in CB, they can be expanded to at least 10^{15} cells and maintain a normal karyotype. In contrast to MSCs from BM (26), the USSCs have a wider differentiation potential and differ in immunophenotype (44) and in their mRNA expression profile. Further differences between MSCs and USSCs include absent expression in USSCs of CD50, CD62L, CD106, and HAS1 (45), all of which are present in MSC. In contrast, USSCs are positive for the epithelial markers cytokeratin 8 and 18 and the endothelial marker KDR. In addition, CD44 was expressed in USSCs but not found on human or rodent MAPCs (12, 13). One major biological difference between USSCs and human MAPCs generated from BM (13) is the ease of generation of USSCs in cytokine-free cultures. The potential to generate hematopoietic cells as shown here from USSCs in vitro and in vivo has not been described for human MAPC. The USSC population can differentiate in vitro into osteoblasts, chondroblasts, adipocytes, and neural cell types in a homogeneous fashion. In these in vitro experiments with a clear, directed differentiation in the initial absence of the target tissue, cell fusion cannot account for the observed differentiation events. Osteogeneic, chondrogeneic, and neural differentiation were documented in vivo and in vitro; however, as shown for neuronal in vitro differentiation, only a precursor-like phenotype was generated which might be explained by the lack of a proper microenvironment with special cytokines and/or molecular signals which are not present in the in vitro culture system. Thus, these specific biological niches are able to fully exploit the intrinsic pluripotentiality of USSCs. Also, the in vivo differentiation of hematopoietic cells, which is seen in a similar quantity as that observed for purified $CD34^+$ from CB (46), could not be confirmed in all experiments in vitro. However, a low frequency of hematopoietic colonies in 2 out of 14 culture experiments with cytokine-primed USSCs was observed. The reason for this in vitro versus in vivo difference cannot be explained yet. The immature mesodermal nature of these cells could be one possible reason: this means that a hematopoietic precursor cell derived from USSCs requires different growth/differentiation conditions, which are present in the in utero fetal sheep model (19).

One major difference compared to human MSCs is the distribution of USSC-derived cells in the heart. In previous studies using the preimmune fetal sheep model, we have shown that human MSCs engraft predominantly in the Purkinje fiber system and there are very few ventricular or atrial cardiomyocytes of human origin (30). In contrast, USSC-derived cells form both Purkinje fiber cells and cardiomyocytes. This would indicate that the USSCs are of an earlier cell type than multipotent MSC, possibly representing also the precursor cell for MSC. The ability of the USSCs to form more than one cell type suggests that these cells may be a valuable source of cells for the repair of the infarcted heart. Future studies will address whether USSCs engraft in other cell types in the heart. Another interesting observation is that the engrafted USSCs, which differentiated into cardiomyocytes, are interspersed with the sheep cardiomyocytes and are thus likely to participate in myocardial function. However similar to the engraftment of human MSCs (30) into the Purkinje fiber system, USSC-derived human cells form aggregates. This could indicate that during fetal development there are different mechanisms of expansion and/or recruitment of cells in the fetus between ventricular or atrial cardiomyocytes and the Purkinje fiber system. Given the remarkably high frequency of human cells in the noninjury transplant model, it was critical to determine whether any of the further differentiation pathways of USSCs into hematopoietic cells, parenchymal liver cells (>20%), and cardiomyocytes could be a result of cell fusion events. Fused cells have been described in the liver and in models of severe injury where the mouse will die if there is not a significant degree of regeneration (11). Because the human sheep chimeric model is a noninjury model, no driving force for potential fusion would exist apriori. As shown recently by Alvarez-Dolado et al. (47) in a noninjury mouse model using the Cre/lox system after BM transplantation, the frequency of newly generated tissue-specific cells in brain, heart, and liver resulting from fusion with respective tissue-specific cells after 10 mo at maximum was only 2.95 fused cells per section in the liver and 2.84 fused cells per section in the heart, respectively. This low frequency would hardly justify attributing fusion as the major or principal mechanism for the de novo generation of organ-specific cells. In contrast, in analyzing fusion versus nonfusion events the data shown here applying the noninjury in utero sheep model document a substantial degree of USSC-differentiated human parenchymal liver cells/slide in the liver and the heart. In the chimeric sheep liver, no indication of cell fusion was detectable. Therefore, the de novo generation of liver and heart cells from certain immature somatic progenitors appear predominantly engaged in noninjury organ regeneration. Importantly, the application of USSCs into different species thus far has not induced macroscopic or microscopic tumors month or even years (in sheep) after transplantation. In addition, USSCs lack HLA class II and costimulatory molecule expression. Preliminary experiments such as mixed culture inhibition suggest that USSCs, similar to adult and fetal MSCs (48), are also nonimmunogeneic and could even be immunosuppressive. This issue is under further investigation.

Thus, on the basis of their pluripotency and expansion under GMP conditions into large quantities, these USSC, when pretested for infectious agents and matched for the

major transplantation antigens, may serve as a universal allogeneic stem cell source for the future development of cellular therapy for tissue repair and tissue regeneration.

We gratefully acknowledge the expert performance of electrophysiological experiments by Prof. K. Gottmann and A. Copi from the Department of Neurophysiology at the University of Düsseldorf, Germany, and are indebted to Anja Mottok and Martin-Leo Hansmann (Department for Pathology, University of Frankfurt, Germany) for sharing their expertise in single cell micromanipulation with us.

The work was supported by grants from the Stem Cell Network North Rhine-Westphalia and Eurocord III, and the National Institutes of Health grants AR45112 and HL077976.

Submitted: 8 March 2004
Accepted: 19 May 2004

References

1. Kuehnle, I., and M.A. Goodell. 2002. The therapeutic potential of stem cells from adults. *BMJ*. 325:372–376.
2. Thomson, J.A., J. Itskovitz-Eldor, S.S. Shapiro, M.A. Waknitz, J.J. Swiergiel, V.S. Marshall, and J.M. Jones. 1998. Embryonic stem cell lines derived from human blastocysts. *Science*. 282:1145–1147.
3. Erdo, F., C. Buhrle, J. Blunk, M. Hoehn, Y. Xia, B. Fleischmann, M. Focking, E. Kustermann, E. Kolossov, J. Hescheler, et al. 2003. Host-dependent tumorigenesis of embryonic stem cell transplantation in experimental stroke. *J. Cereb. Blood Flow Metab*. 23:780–785.
4. Sapienza, C. 2002. Imprinted gene expression, transplantation medicine, and the "other" human embryonic stem cell. *Proc. Natl. Acad. Sci. USA*. 99:10243–10245.
5. Gussoni, E., Y. Soneoka, C.D. Strickland, E.A. Buzney, M.K. Khan, A.F. Flint, L.M. Kunkel, and R.C. Mulligan. 1999. Dystrophin expression in the mdx mouse restored by stem cell transplantation. *Nature*. 401:390–394.
6. Petersen, B.E., W.C. Bowen, K.D. Patrene, W.M. Mars, A.K. Sullivan, N. Murase, S.S. Boggs, J.S. Greenberger, and J.P. Goff. 1999. Bone marrow as a potential source of hepatic oval cells. *Science*. 284:1168–1170.
7. Mezey, E., K.J. Chandross, G. Harta, R.A. Maki, and S.R. McKercher. 2000. Turning blood into brain: cells bearing neuronal antigens generated in vivo from bone marrow. *Science*. 290:1779–1782.
8. Krause, D.S., N.D. Theise, M.I. Collector, O. Henegariu, S. Hwang, R. Gardner, S. Neutzel, and S.J. Sharkis. 2001. Multi-organ, multi-lineage engraftment by a single bone marrow-derived stem cell. *Cell*. 105:369–377.
9. Korbling, M., R.L. Katz, A. Khanna, A.C. Ruifrok, G. Rondon, M. Albitar, R.E. Champlin, and Z. Estrov. 2002. Hepatocytes and epithelial cells of donor origin in recipients of peripheral-blood stem cells. *N. Engl. J. Med*. 346:738–746.
10. Wagers, A.J., R.I. Sherwood, J.L. Christensen, and I.L. Weissman. 2002. Little evidence for developmental plasticity of adult hematopoietic stem cells. *Science*. 297:2256–2259.
11. Wang, X., H. Willenbring, Y. Akkari, Y. Torimaru, M. Foster, M. Al-Dhalimy, E. Lagasse, M. Finegold, S. Olson, and M. Grompe. 2003. Cell fusion is the principal source of bone-marrow-derived hepatocytes. *Nature*. 422:897–901.
12. Jiang, Y., B.N. Jahagirdar, R.L. Reinhardt, R.E. Schwartz, C.D. Keene, X.R. Ortiz-Gonzalez, M. Reyes, T. Lenvik, T. Lund, M. Blackstad, et al. 2002. Pluripotency of mesenchymal stem cells derived from adult marrow. *Nature*. 418:41–49.
13. Reyes, M., T. Lund, T. Lenvik, D. Aguiar, L. Koodie, and C.M. Verfaillie. 2001. Purification and ex vivo expansion of postnatal human marrow mesodermal progenitor cells. *Blood*. 98:2615–2625.
14. Geiger, H., and G. Van Zant. 2002. The aging of lympho-hematopoietic stem cells. *Nat. Immunol*. 3:329–333.
15. Mendes, S.C., J.M. Tibbe, M. Veenhof, K. Bakker, S. Both, P.P. Platenburg, F.C. Oner, J.D. De Bruijn, and C.A. Van Blitterswijk. 2002. Bone tissue-engineered implants using human bone marrow stromal cells: effect of culture conditions and donor age. *Tissue Eng*. 8:911–920.
16. Szilvassy, S.J., T.E. Meyerrose, P.L. Ragland, and B. Grimes. 2001. Differential homing and engraftment properties of hematopoietic progenitor cells from murine bone marrow, mobilized peripheral blood, and fetal liver. *Blood*. 98:2108–2115.
17. Vaziri, H., W. Dragowska, R.C. Allsopp, T.E. Thomas, C.B. Harley, and P.M. Lansdorp. 1994. Evidence for a mitotic clock in human hematopoietic stem cells: loss of telomeric DNA with age. *Proc. Natl. Acad. Sci. USA*. 91:9857–9860.
18. Migliaccio, G., A.R. Migliaccio, S. Petti, F. Mavilio, G. Russo, D. Lazzaro, U. Testa, M. Marinucci, and C. Peschle. 1986. Human embryonic hemopoiesis. Kinetics of progenitors and precursors underlying the yolk sac-liver transition. *J. Clin. Invest*. 78:51–60.
19. Zanjani, E.D., J.L. Ascensao, and M. Tavassoli. 1993. Liver-derived fetal hematopoietic stem cells selectively and preferentially home to the fetal bone marrow. *Blood*. 81:399–404.
20. Rubinstein, P., R.E. Rosenfield, J.W. Adamson, and C.E. Stevens. 1993. Stored placental blood for unrelated bone marrow reconstitution. *Blood*. 81:1679–1690.
21. Kogler, G., J. Callejas, P. Hakenberg, J. Enczmann, O. Adams, W. Daubener, C. Krempe, U. Gobel, T. Somville, and P. Wernet. 1996. Hematopoietic transplant potential of unrelated cord blood: critical issues. *J. Hematother*. 5:105–116.
22. Harley, C.B., A.B. Futcher, and C.W. Greider. 1990. Telomeres shorten during ageing of human fibroblasts. *Nature*. 345:458–460.
23. Paxinos, G. and C. Watson. 1982. The Rat Brain in Stereotaxic Coordinates. Academic Press, Sydney, Australia.
24. Jaiswal, N., S.E. Haynesworth, A.I. Caplan, and S.P. Bruder. 1997. Osteogenic differentiation of purified, culture-expanded human mesenchymal stem cells in vitro. *J. Cell. Biochem*. 64: 295–312.
25. Johnstone, B., T.M. Hering, A.I. Caplan, V.M. Goldberg, and J.U. Yoo. 1998. In vitro chondrogenesis of bone marrow-derived mesenchymal progenitor cells. *Exp. Cell Res*. 238:265–272.
26. Pittenger, M.F., A.M. Mackay, S.C. Beck, R.K. Jaiswal, R. Douglas, J.D. Mosca, M.A. Moorman, D.W. Simonetti, S. Craig, and D.R. Marshak. 1999. Multilineage potential of adult human mesenchymal stem cells. *Science*. 284:143–147.
27. Bruder, S.P., N. Jaiswal, N.S. Ricalton, J.D. Mosca, K.H. Kraus, and S. Kadiyala. 1998. Mesenchymal stem cells in osteobiology and applied bone regeneration. *Clin. Orthop*. 355:S247-S256.
28. Ponticiello, M.S., R.M. Schinagl, S. Kadiyala, and F.P. Barry. 2000. Gelatin-based resorbable sponge as a carrier matrix for human mesenchymal stem cells in cartilage regeneration therapy. *J. Biomed. Mater. Res*. 52:246–255.
29. Kogler, G., J. Callejas, R.V. Sorg, J. Fischer, A.R. Migliaccio, and P. Wernet. 1998. The effect of different thawing methods, growth factor combinations and media on the ex

vivo expansion of umbilical cord blood primitive and committed progenitors. *Bone Marrow Transplant*. 21:233–241.
30. Airey, J.A., G. Almeida-Porada, E.J. Colletti, C.D. Porada, J. Chamberlain, M. Movsesian, J.L. Sutko, and E.D. Zanjani. 2004. Human mesenchymal stem cells from purkinje fibers in fetal sheep heart. *Circulation*. 109:1401–1407.
31. Klein, F., N. Feldhahn, S. Lee, H. Wang, F. Ciuffi, M. von Elstermann, M.L. Toribio, H. Sauer, M. Wartenberg, V.S. Barath, et al. 2003. T lymphoid differentiation in human bone marrow. *Proc. Natl. Acad. Sci. USA*. 100:6747–6752.
32. Schousboe, A., and D.A. Redburn. 1995. Modulatory actions of gamma aminobutyric acid (GABA) on GABA type A receptor subunit expression and function. *J. Neurosci. Res*. 41:1–7.
33. Allay, J.A., J.E. Dennis, S.E. Haynesworth, M.K. Majumdar, D.W. Clapp, L.D. Shultz, A.I. Caplan, and S.L. Gerson. 1997. LacZ and interleukin-3 expression in vivo after retroviral transduction of marrow-derived human osteogenic mesenchymal progenitors. *Hum. Gene Ther*. 8:1417–1427.
34. Flake, A.W., M.R. Harrison, N.S. Adzick, and E.D. Zanjani. 1986. Transplantation of fetal hematopoietic stem cells in utero: the creation of hematopoietic chimeras. *Science*. 233:776–778.
35. Zanjani, E.D., A.W. Flake, H. Rice, M. Hedrick, and M. Tavassoli. 1994. Long-term repopulating ability of xenogeneic transplanted human fetal liver hematopoietic stem cells in sheep. *J. Clin. Invest*. 93:1051–1055.
36. Leger, J.P., F.M. Smith, and R.W. Currie. 2000. Confocal microscopic localization of constitutive and heat shock-induced proteins HSP70 and HSP27 in the rat heart. *Circulation*. 102:1703–1709.
37. Chevron, M.P., F. Girard, M. Claustres, and J. Demaille. 1994. Expression and subcellular localization of dystrophin in skeletal, cardiac and smooth muscles during the human development. *Neuromuscul. Disord*. 4:419–432.
38. Torelli, S., A. Ferlini, L. Obici, C. Sewry, and F. Muntoni. 1999. Expression, regulation and localisation of dystrophin isoforms in human foetal skeletal and cardiac muscle. *Neuromuscul. Disord*. 9:541–551.
39. Erices, A., P. Conget, and J.J. Minguell. 2000. Mesenchymal progenitor cells in human umbilical cord blood. *Br. J. Haematol*. 109:235–242.
40. Romanov, Y.A., V.A. Svintsitskaya, and V.N. Smirnov. 2003. Searching for alternative sources of postnatal human mesenchymal stem cells: candidate MSC-like cells from umbilical cord. *Stem Cells*. 21:105–110.
41. Goodwin, H.S., A.R. Bicknese, S.N. Chien, B.D. Bogucki, C.O. Quinn, and D.A. Wall. 2001. Multilineage differentiation activity by cells isolated from umbilical cord blood: expression of bone, fat, and neural markers. *Biol. Blood Marrow Transplant*. 7:581–588.
42. Wexler, S.A., C. Donaldson, P. Denning-Kendall, C. Rice, B. Bradley, and J.M. Hows. 2003. Adult bone marrow is a rich source of human mesenchymal 'stem' cells but umbilical cord and mobilized adult blood are not. *Br. J. Haematol*. 121: 368–374.
43. Mareschi, K., E. Biasin, W. Piacibello, M. Aglietta, E. Madon, and F. Fagioli. 2001. Isolation of human mesenchymal stem cells: bone marrow versus umbilical cord blood. *Haematologica*. 86:1099–1100.
44. Deans, R.J., and A.B. Moseley. 2000. Mesenchymal stem cells: biology and potential clinical uses. *Exp. Hematol*. 28: 875–884.
45. Nilsson, S.K., D.N. Haylock, H.M. Johnston, T. Occhiodoro, T.J. Brown, and P.J. Simmons. 2003. Hyaluronan is synthesized by primitive hemopoietic cells, participates in their lodgment at the endosteum following transplantation, and is involved in the regulation of their proliferation and differentiation in vitro. *Blood*. 101:856–862.
46. Lewis, I.D., G. Almeida-Porada, J. Du, I.R. Lemischka, K.A. Moore, E.D. Zanjani, and C.M. Verfaillie. 2001. Umbilical cord blood cells capable of engrafting in primary, secondary, and tertiary xenogeneic hosts are preserved after ex vivo culture in a noncontact system. *Blood*. 97:3441–3449.
47. Alvarez-Dolado, M., R. Pardal, J.M. Garcia-Verdugo, J.R. Fike, H.O. Lee, K. Pfeffer, C. Lois, S.J. Morrison, and A. Alvarez-Buylla. 2003. Fusion of bone-marrow-derived cells with Purkinje neurons, cardiomyocytes and hepatocytes. *Nature*. 425:968–973.
48. Le Blanc, K. 2003. Immunomodulatory effects of fetal and adult mesenchymal stem cells. *Cytotherapy*. 5:485–489.
49. Zanjani, E.D., E.F. Srour, and R. Hoffman. 1995. Retention of long-term repopulating ability of xenogeneic transplanted purified adult human bone marrow hematopoietic stem cells in sheep. *J. Lab. Clin. Med*. 126:24–28.